

# Ionic contribution to the dielectric properties of a nematic liquid crystal in thin cells

Surajit Dhara and N. V. Madhusudana<sup>a)</sup>

Raman Research Institute, C. V. Raman Avenue, Bangalore 560 080, India

(Received 9 January 2001; accepted for publication 1 June 2001)

We report measurements on dielectric properties of a nematic liquid crystal in planar aligned cells with two different thicknesses (1.2 and 6.7  $\mu\text{m}$ ). The nematic has a wide thermal range and the temperature variation of the effective dielectric constant ( $\epsilon_{\perp}$ ) of the thick cell reflects that of the orientational order parameter. On the other hand, the thin cell exhibits a higher value of  $\epsilon_{\perp}$  which is essentially temperature independent. We have conducted detailed dielectric measurements in the frequency range of 10 Hz–1.1 kHz on both the cells and analyzed the data using a simplified model which takes into account the ionic contribution. It leads to an estimation of the temperature dependencies of the number density and diffusion coefficient of the impurity ions. © 2001 American Institute of Physics. [DOI: 10.1063/1.1388163]

## I. INTRODUCTION

Nematic (*N*) liquid crystals are orientationally ordered liquids, made of rod-like organic molecules.<sup>1</sup> The average orientation direction of the molecules is specified by a unit vector  $\hat{n}$  called the director which is *apolar* in nature. The medium combines anisotropies in dielectric, optical, and other properties with a facility to flow and hence exhibits pronounced electro-optic effects, which are exploited in flat panel liquid crystal display (LCD) devices.<sup>2</sup> The chemical compound exhibiting the nematic itself is usually a good insulator. However, unless special precautions are taken, the material has ionic impurities, giving rise to an electrical conductivity  $\sigma \sim 10^{-10} (\Omega \text{ cm})^{-1}$ . The conductivity has positive anisotropy  $\Delta\sigma = \sigma_{\parallel} - \sigma_{\perp}$ , in which the subscripts refer to directions in relation to  $\hat{n}$ . Indeed in materials with negative dielectric anisotropy  $\Delta\epsilon$ , a dc or low frequency ac electric voltage beyond a threshold value can generate electrohydrodynamic (EHD) instabilities, due to the ionic conductivity.<sup>1</sup> The display devices make use of electric field (*E*) effects in materials with positive  $\Delta\epsilon$ , which favors an alignment of  $\hat{n}$  parallel to *E*. Since a nematic is a liquid, its response is relatively slow,<sup>1</sup> and the response time  $\tau \approx \eta d^2 / \pi^2 K$ , where  $\eta$  is an effective viscosity, *K* an effective curvature elastic constant and *d* the sample thickness. A typical LCD cell has a thickness  $\approx 5 \mu\text{m}$ . The response time can be reduced considerably by reducing the thickness. Furthermore, in the surface stabilized ferroelectric devices,<sup>3</sup> as well as the bistable twisted nematic displays<sup>4,5</sup> which are being investigated in recent years, the thickness has to be quite small,  $\approx 2 \mu\text{m}$  or lower. When the thickness of the sample is reduced, at any given applied voltage the field increases and the influence of ions on the electrical properties of the cell becomes significant. The ionic contribution has been discussed in detail only in the case of EHD instabilities, and on the dc switching process in a boundary layer bistable nematic display.<sup>6</sup>

Dielectric spectroscopy is used to characterize the electrical properties of condensed matter. The influence of ions on the real and imaginary parts of the frequency dependent dielectric constants of both solid and liquid electrolytes has been studied both experimentally and theoretically for a long time.<sup>7–9</sup> The theory has since been extended for polymer melts,<sup>10</sup> which has been subsequently simplified and used to describe the effect of ions on the dielectric response in the isotropic (*I*) phase of liquid crystals.<sup>11,12</sup> The latter studies were made on cells with a thickness of about 5  $\mu\text{m}$  or larger. In view of the emerging interest in using much thinner cells in LCDs, as well as an intrinsic interest in the problem, it would be useful to conduct experiments in much thinner cells, with thickness  $< 2 \mu\text{m}$ . In this article, we report frequency dependence of dielectric properties on a nematogen which exhibits the nematic phase over a very wide temperature range. The measurements have been made on cells with two different thicknesses and indeed the thinner ( $\approx 1.2 \mu\text{m}$ ) cell shows a pronounced influence due to the ionic contribution. In Sec. II, we give the experimental technique, and describe the results and discuss the latter on the basis of an appropriate theoretical model in Sec. III. We make some concluding remarks Sec. IV.

## II. EXPERIMENT

The main aim of this investigation is to look for the influence of ions on dielectric properties of liquid crystals. In the display devices, the liquid crystal is aligned with its director parallel to the glass plates. The dielectric anisotropy ( $\Delta\epsilon$ ) of the material is positive so that the nematic shows a realignment of the director above a threshold voltage<sup>2</sup> (Fredericksz transition). We have chosen a material with negative dielectric anisotropy to avoid this problem. However, such a material can give rise to EHD instabilities beyond a threshold of about  $\approx 5 \text{ V}$  or more, depending on the frequency.<sup>1</sup> We conduct our experiments at 1 V which is well below the threshold value. The compound studied is 2-cyano 4-heptylphenyl-4'-pentyl-4-biphenyl carboxylate [7(CN)5

<sup>a)</sup>Electronic mail: nvmadhu@rri.res.in

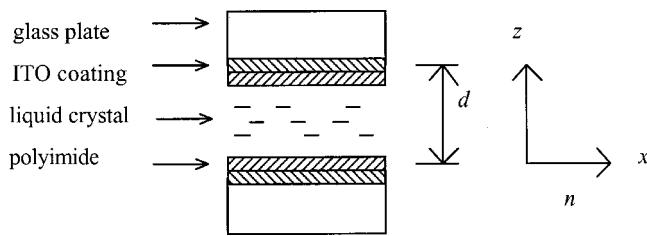


FIG. 1. Schematic diagram of the planar aligned nematic liquid crystal cell used in the experiments. Note that the gap  $d$  is highly exaggerated for clarity.

for short] which has the phase sequence: crystal 45 °C N 102 °C I. It was obtained from Merck. The lateral cyano group of the molecule gives rise to a large negative dielectric anisotropy in the nematic phase.<sup>13</sup> The material has a very wide nematic range and the liquid crystal can be easily supercooled to room temperature. It is also chemically stable. The cells (Fig. 1) were prepared using 0.5 mm thick indium tin oxide (ITO) coated glass plates. An appropriate pattern was etched in the two plates so that the cell had an overlapping ITO (i.e., electrode) area  $a$  of 0.6 cm<sup>2</sup>. The etched plates were coated with a polyimide layer and cured at 280 °C for 1 h. The coating was then rubbed unidirectionally with a tissue paper. The plates of the cell were separated by appropriate spherical spacers and sealed with a glue. The rubbing directions on the two plates were arranged to be parallel to ensure a planar alignment of the liquid crystal. The thickness  $d$  of the empty cell was measured using channel spectrum. Two thicknesses viz.,  $d=6.7 \mu\text{m}$  and  $d=1.2 \mu\text{m}$  were chosen for the studies. The cells were filled with the sample in the isotropic phase and on slow cooling to the nematic range, well aligned samples were obtained. The electrical connections to the two plates were made through copper wires which were soldered to the appropriate connection pads using an ultrasonic soldering gun.

The temperature of the sample was maintained and measured (to  $\sim 10$  mK) by placing it in an Instec hot stage. The dielectric properties of the cell were measured using a DSP lock-in amplifier (SRS 830). The block diagram of the setup is shown in Fig. 2. The sinusoidal output of the internal

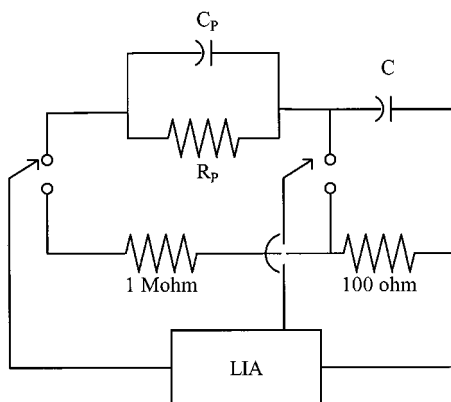


FIG. 2. Block diagram of the experimental setup used for the impedance analysis of the liquid crystal cell. LIA is an SRS 830 lock-in amplifier. The voltage across the capacitance  $C(=1 \mu\text{F})$  is used in the impedance analysis.

oscillator of the lock-in amplifier is adjusted to a rms value of 1 V, and applied to the cell which is in series with a  $1 \mu\text{F}$  standard capacitor ( $C$ ) as shown in the figure. The amplitude and phase of the applied voltage are also checked using a reference circuit with two standard resistors in series, connected in place of the cell. The phase ( $\phi$ ) and the rms amplitude ( $V$ ) of the voltage measured across the series  $1 \mu\text{F}$  capacitor are used to calculate the capacitance and parallel resistance corresponding to the cell by using the following relations:<sup>14</sup>

$$R_p = \frac{Y}{\omega \sin \alpha}$$

$$C_p = \frac{X}{Y}, \quad (1)$$

where  $X = \cos \alpha - Q$ ,  $Y = (\sin^2 \alpha + X^2)/CQ$ ,  $Q = V/V_0$ , and  $\alpha = \psi - \phi$  where  $V_0$  and  $\psi$  are the amplitude and phase and  $\omega$  the angular frequency of the applied signal.

We have checked the calibration of the setup by connecting standard capacitors in parallel with standard resistors in place of the liquid crystal cell. The measured values agree with the standard values to within  $\sim 3\%$ . We have also checked the calibration by measuring the capacitance and resistance using a Wayne-Kerr bridge which operates at 1.6 kHz.

The measurements were completely controlled by a computer, using a suitable program. The temperature was maintained at various values in the nematic range to an accuracy of  $\pm 0.01$  °C, and the measurements were made at several frequencies in the range of 10–1100 Hz.

### III. RESULTS AND DISCUSSION

In order to bring out the strong influence of the cell thickness on the measured properties, we have shown the effective dielectric constant [which is the ratio of the cell capacitance with the sample ( $C_p$ ) to that of the empty cell] and conductivity at 1.1 kHz as functions of temperature for both the cells in Figs. 3 and 4, respectively. These measurements correspond to  $\epsilon_{\perp}$  and  $\sigma_{\perp}$ , i.e., the properties in a direction orthogonal to the director. In Fig. 3, the dielectric constant of the  $6.7 \mu\text{m}$  thick cell follows the expected trend, decreasing with increase of temperature, the rate of decrease becoming rapid near the nematic–isotropic transition point  $T_{NI}$ . It is easily shown that<sup>1</sup> the contribution from the liquid crystal is given by:

$$\epsilon_{\perp} = \bar{\epsilon} - \frac{1}{3} \delta \epsilon S, \quad (2)$$

where  $[\bar{\epsilon} = (\epsilon_{\parallel} + 2\epsilon_{\perp})/3]$  is the average dielectric constant, and  $\delta \epsilon$  is the value of the anisotropy ( $\Delta \epsilon$ ) when the order parameter  $S = 1$ . As  $S$  decreases with increase of temperature, and  $\delta \epsilon$  is negative,  $\epsilon_{\perp}$  decreases with temperature. The trend shown by the thin cell is peculiar. The dielectric constant is somewhat larger than that for the thicker cell even at low temperatures, but at temperatures above 60 °C, the value does not decrease as in the thicker cell but more or less remains constant and decreases slightly only very near  $T_{NI}$ . In both cases, the dielectric constant jumps to a lower value

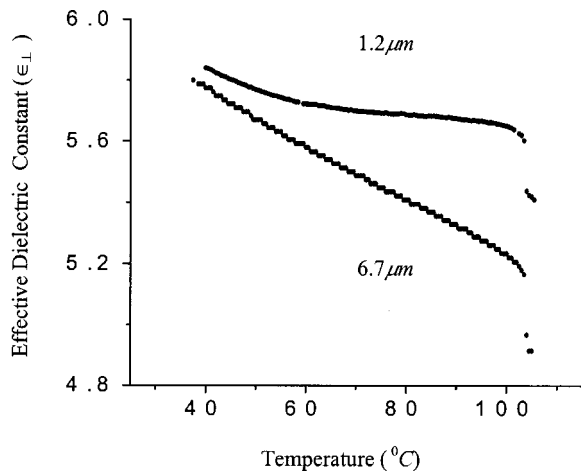


FIG. 3. Temperature dependence of the effective dielectric constant of the liquid crystal taken in cells with two different thicknesses, at a frequency of 1.1 kHz. Note the higher value for the thinner cell, which hardly varies with temperature in the nematic phase above 60 °C.

at  $T_{NI}$ . Furthermore, the value for the thinner cell continues to be significantly larger than that for the thicker one even in the isotropic phase.

The effective conductivity given by  $\sigma_{\perp} = d/(aR_p)$  is shown in Fig. 4 for both the cells. As expected, the conductivity increases with temperature in both cases as the mobility and the number density of ions increase with temperature. However, it can be noted that the relative variation of  $\sigma_{\perp}$  in the thin cell is somewhat higher than that in the thick cell.

The markedly different response of the thin cell compared to the thick one arises due to the ionic contribution. In order to investigate this effect in greater detail, we have carried out frequency dependent measurements of the dielectric properties at different temperatures. The raw data on the effective dielectric constant and conductivity are not convenient for a comparison with the theoretical analysis to follow. We first present a summary of the theoretical background.

The liquid crystal is separated by the ITO electrodes by aligning polyimide layers as in LCDs (see Fig. 1). This

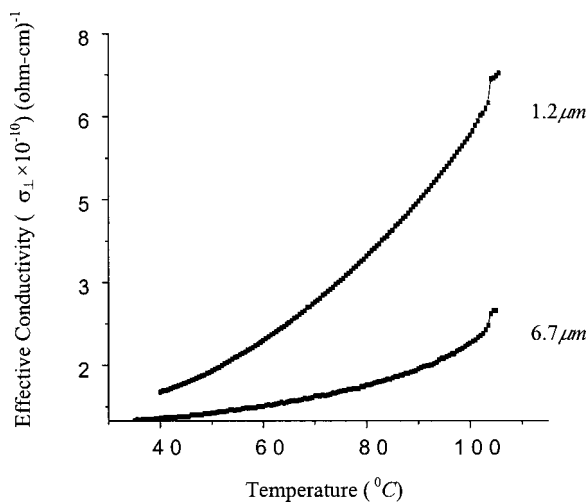


FIG. 4. Temperature dependence of the effective conductivity of the liquid crystal in the two cells as described in the caption of Fig. 3.

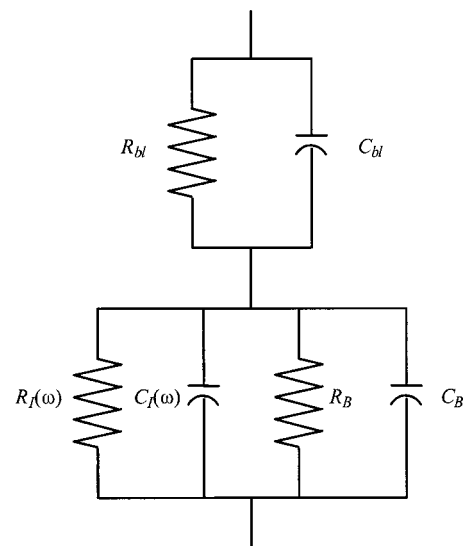


FIG. 5. Equivalent circuit of the liquid crystal cell with the “lumped” values of the boundary layer capacitance  $C_{bl}$  and resistance  $R_{bl}$  arising from both the boundaries.

boundary layer has a typical thickness of few hundred Å and its effective electrical resistance ( $R_{bl}$ ) as well as capacitance ( $C_{bl}$ ) can be expected to be quite large, i.e., the layer essentially is an insulator. As the dielectric constant of this layer is similar to that of the liquid crystal, it can be assumed that there is no adsorption of ions at the interface between the two. The dielectric constant ( $\epsilon_{\perp}$ ) of the liquid crystal medium itself, which depends on the induced dipole and orientation polarization contributions of the molecules can be considered to be essentially frequency independent in the range ( $<1.5$  kHz) in which the measurements have been made. This contribution produces an effective bulk capacitance denoted by  $C_B$ . The medium also has a uniform distribution of ions, which produces a frequency independent conductivity  $\sigma$  which in turn produces a bulk resistance of the medium denoted by  $R_B$ . The application of an electric field generates a nonuniform distribution of ions which depends on the frequency and in turn contributes both to the real and imaginary parts of the dielectric constant. These in turn give rise to a capacitance  $C_f(\omega)$  and resistance  $R_f(\omega)$ . The equivalent circuit corresponding to the cell in which all these contributions have been included is shown in Fig. 5. The complex impedance of the equivalent circuit is given by<sup>11</sup>

$$Z_A = \frac{2R_{bl}}{1 + (\omega R_{bl}C_{bl})^2} + \frac{\frac{1}{R_B} + \frac{1}{R_f(\omega)}}{\left[\frac{1}{R_B} + \frac{1}{R_f(\omega)}\right]^2 + \omega^2[C_B + C_f(\omega)]^2} - j \left[ \frac{2\omega R_{bl}^2 C_{bl}}{1 + (\omega R_{bl}C_{bl})^2} + \frac{\omega[C_B + C_f(\omega)]}{\left[\frac{1}{R_B} + \frac{1}{R_f(\omega)}\right]^2 + \omega^2[C_B + C_f(\omega)]^2} \right]. \quad (3)$$

In terms of the measured values  $C_p$  and  $R_p$  [given by Eq. (1)], the *measured* complex impedance is given by

$$Z_B = \frac{R_p}{1 + (\omega R_p C_p)^2} - j \left[ \frac{\omega R_p^2 C_p}{1 + (\omega R_p C_p)^2} \right]. \quad (4)$$

We summarize below a grossly simplified method of evaluation of the ionic contribution which generates  $C_I(\omega)$  and  $R_I(\omega)$ . It is convenient to assume that positive ions are very much more mobile than the negative ones and the latter do not contribute to the current. If  $\rho(z,t)$  is the charge density of the mobile ions, the charge continuity equation is given by

$$\frac{\partial \rho}{\partial t} + \frac{\partial J(z,t)}{\partial z} = 0, \quad (5)$$

where  $J(z,t)$  is the current density, which is given by

$$J(z,t) = -D \frac{\partial \rho(z,t)}{\partial z} + \mu \rho(z,t) E e^{i\omega t}, \quad (6)$$

where  $D$  is the diffusion constant and  $\mu$  is the mobility. As the polyimide is a blocking layer, we can assume that at the two boundaries ( $z=0$  and  $d$ )  $J_{(0)} = J_{(d)} = 0$ . As our measurements have been made only at the frequency  $\omega$  of the applied voltage, we assume that

$$\rho(z,t) = \rho_0(z) + \rho_1(z) e^{i\omega t}, \quad (7)$$

where  $\rho_0(z)$  is the time independent density of ions and  $\rho_1(z)$  is the amplitude of ion density which oscillates at the frequency of the applied field. The mobile charges move under the action of the external field and the resulting space charges produce a polarization which contributes to the total dielectric constant. The space charges give rise to a nonuniform electric field which can be calculated by using the Poisson relation. The solutions in that case are quite complicated and cannot be expressed in a simple analytical form. Our sample had unknown ionic species whose number density ( $n$ ) is  $\sim 10^{15}/\text{cc}$ . As such, the sample is really a *weak* electrolyte. Furthermore, the transit time of ions from one electrode to the other under a reversal of a voltage  $V$  is given by  $\tau_{tr} = (6\pi\eta r/q)(d^2/V)$  where  $\eta$  the effective viscosity is  $\approx 1$  poise at room temperature, and  $r$  the ionic radius can be expected to be  $\sim 10 \text{ \AA}$ . However, as the mesogenic molecules are strongly polar we can also expect that the ion will be dressed by a few molecules which are attached to the ion. The effective "ionic" radius can be a few (say  $\sim 5$ ) times larger than the bare value. For the thick cell,  $\tau_{tr} \approx 2$  s while it is about 0.1 s for the thinner one for the applied voltage of 1 V. As such, in the frequency range of interest (10–1100 Hz), to a good approximation, the nonuniformity in ion distribution can be assumed to be small. The field in the cell can then be assumed to be equal to the external field. As the temperature is increased, the viscosity reduces and the approximation becomes less justifiable. However use of the approximation has the virtue that analytical expressions can be derived for  $C_I(\omega)$  and  $R_I(\omega)$ . In a recent paper Sawada *et al.*<sup>12</sup> have also argued that the approximation may be adequate. Moreover, we can fit the experimental data quite well to the solutions by using this approximation, which is hence further justified *a posteriori*. Using the boundary condition that  $J = 0$  it can be shown that  $\rho_0$  is actually independent of  $z$  and

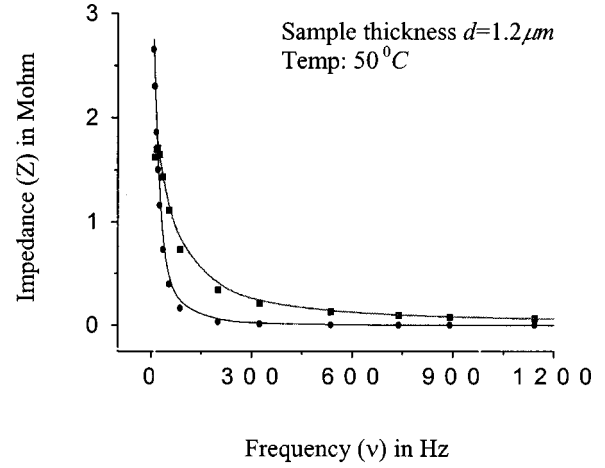


FIG. 6. Temperature dependencies of the real (filled circles) and the imaginary (filled squares) parts of the measured impedance  $Z_B$  [see Eq. (4)] in the cell with thickness  $1.2 \mu\text{m}$ , at  $50^\circ\text{C}$ . The lines show the calculated variations of  $Z_A$  [see Eq. (3)] with the fit parameters shown in Table Ia.

$$\rho_1(z) = \frac{\mu E}{\kappa D} \rho_0 \left( \frac{e^{\kappa z}}{1 + e^{\kappa d}} - \frac{e^{-\kappa z}}{1 + e^{-\kappa d}} \right), \quad (8)$$

where  $\kappa = \sqrt{i\omega/D}$  and from the Einstein relation,  $\mu/D = q/k_B T$ , where  $k_B$  is the Boltzmann constant. Hence  $\rho_1(z)$  has components both in phase and  $\pi/2$  out of phase with the applied ac field. The additional polarization due to the space charge formation is  $[\rho_1(z)z]$  and the thickness averaged value is

$$\bar{P}(t) = e^{i\omega t} \frac{\int_0^d \rho_1(z) dz}{\int_0^d dz}. \quad (9)$$

The corresponding frequency-dependent ionic contributions to the complex dielectric constant are given by:

$$\frac{C_I(\omega)d}{\epsilon_0 a} = \epsilon'_I(\omega) = - \left[ \frac{4\pi n q^2 D}{\omega k_B T A} \right] \left[ \frac{1 + 2e^A \sin(A) - e^{2A}}{1 + 2e^A \cos(A) + e^{2A}} \right] \quad (10)$$

and

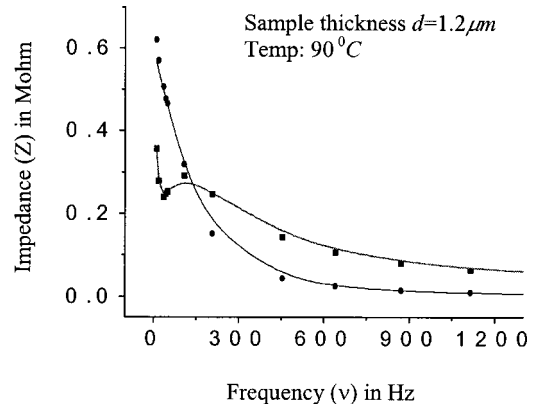


FIG. 7. Same as in Fig. 6, at a temperature of  $90^\circ\text{C}$ . Note the minimum and maximum in the frequency dependence of the imaginary part of the impedance.

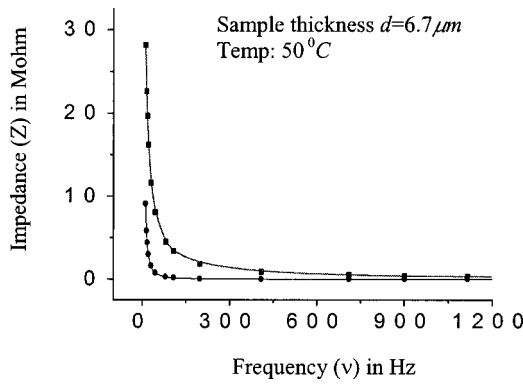


FIG. 8. Same as in Fig. 6, for the thicker cell with  $d=6.7 \mu\text{m}$ , at  $50^\circ\text{C}$ .

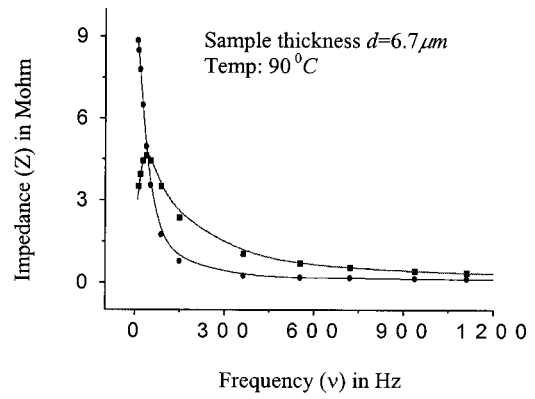


FIG. 9. Same as in Fig. 8 at  $90^\circ\text{C}$ . Note the peak in the frequency dependence of the imaginary part of the impedance.

$$\frac{d}{\omega \epsilon_0 R_l(\omega) a} = \epsilon_l''(\omega) = \frac{4 \pi n q^2 D}{\omega k_B T} \left[ 1 + \frac{1 - 2e^A \sin A - e^{2A}}{A(1 + e^A \cos A + e^{2A})} \right], \quad (11)$$

where  $a$  is the area of electrodes,  $nq = \rho_0$  and  $A = d\sqrt{\omega/2D}$ . Equations (10) and (11) agree with those derived by Sawada.<sup>11</sup> Using these in Eq. (3), the real and imaginary parts of  $Z_A$  can now be calculated. Comparing them with the corresponding parts of the experimental complex impedance  $Z_B$  given by Eq. (4), a nonlinear least-squares fitting procedure is used to get the best values for  $R_{bl}$ ,  $C_{bl}$ ,  $D$ ,  $n$  and the frequency independent terms  $R_B$  and  $C_B$ . Some representative variations of the real and imaginary parts of the impedance are shown in Figs. 6–9 at two different temperatures for both the thin and thick samples. It is seen that the agreement between the calculated and measured variations is quite satisfactory. The relevant fit parameters at different temperatures are collected in Table I for both the thick and thin samples. From the figures it is clear that the real part of  $Z_B$ , which gives the experimental data has a monotonic decrease as a function of frequency at all temperatures for the cells of both thicknesses. The calculated values, which are the real

part of  $Z_A$  agree well with the data. The imaginary part of (the measured)  $Z_B$ , and the corresponding calculations based on  $Z_A$ , show a peak around 100 Hz, which is more pronounced for the thin cell. The frequency corresponding to the peak decreases as the temperature is lowered, while the magnitude of the impedance itself increases. In the thin cell there is also a low frequency minimum above  $75^\circ\text{C}$  and the impedance strongly increases at very low frequencies. The physical origin of these features can be understood from Eqs. (3), (4), (10) and (11).  $A = d\sqrt{\omega/2D}$ , i.e.,  $A \propto \nu^{1/2}$  where  $\nu = \omega/2\pi$  and the lowest frequency that we have used is  $\nu = 10$  Hz. As the typical diffusion constant  $D \sim 10^{-7} \text{ cm}^2/\text{s}$ ,  $A$  is much larger than 1 even for the thin cell. The boundary layer capacitance  $C_{bl}$  is  $\approx 10^{-7}$  F, and the corresponding resistance  $R_{bl} \approx 10^7 \Omega$ . Using these, the imaginary part of  $Z_A$  can be approximated to  $Z_A(\text{imag}) \approx C_1/\omega + [C_2\omega/(1 + C_3\omega^2)]$ , where  $C_1 \sim 10^7$ ,  $C_2 \sim 10^4$  and  $C_3 \sim 10^{-6}$ . It is clear that the second term leads to a maximum when  $\omega^2 = 1/C_3$  where  $\sqrt{C_3}$  is essentially the charge relaxation time  $\epsilon_0 \epsilon_{\perp} / \sigma$ . On the other hand,  $C_1$  arises from the boundary layer impedance and the first term becomes comparable to the second one for  $\omega \approx 100$  (i.e.,  $\nu \approx 20$  Hz). Below this fre-

TABLE I. Fit parameters at different temperatures.

(a) Sample thickness $d = 1.2 \mu\text{m}$						
Temperature in $^\circ\text{C}$	Diffusion constant $D$ ( $\text{cm}^2/\text{s}$ ) ( $\times 10^{-8}$ )	Number density $n$ ( $\text{cc})^{-1}(\times 10^{14})$	Boundary layer resistance $R_{bl}$ (M $\Omega$ )	Boundary layer capacitance $C_{bl}(\times 10^{-7} \text{ F})$	Bulk resistance $R_B$ (M $\Omega$ )	Bulk capacitance $C_B(\times 10^{-9} \text{ F})$
105	6.3	20	7	2.7	1.5	2.1
90	4.9	16	7	2.7	3.4	2.1
65	2.5	6.6	7	2.7	3.2	2.2
50	1.9	4.5	7	2.7	8.5	2.4
(b) Sample thickness $d = 6.7 \mu\text{m}$						
Temperature in $^\circ\text{C}$	Diffusion constant $D$ ( $\text{cm}^2/\text{s}$ ) ( $\times 10^{-8}$ )	Number density $n$ ( $\text{cc})^{-1}(\times 10^{14})$	Boundary layer resistance $R_{bl}$ (M $\Omega$ )	Boundary layer capacitance $C_{bl}(\times 10^{-8} \text{ F})$	Bulk resistance $R_B$ (M $\Omega$ )	Bulk capacitance $C_B(\times 10^{-10} \text{ F})$
105	9.7	4.8	12	9	12	3.8
90	8.8	2.5	12	9	50	4.2
65	6.1	0.6	12	9	83	4.4
50	5.4	0.2	13	9	145	4.7

quency the contribution from the boundary layer leads to a rapid increase in  $Z_A(\text{imag})$  and hence produces the sharp minimum seen in Fig. 7.

From Table I, the number density of ions at any given temperature is much larger in the thin cell compared to the thick one, which arises due to the fact that the two cells were prepared on different days and the contamination during processing of the cells is likely to be responsible for the different values. One can assume that the bulk conductivity  $\sigma \approx \mu\rho$  and the values of the bulk resistivity  $R_B$  are consistent with the diffusion constant  $D$  and the number density  $n$  in both cells. Both decrease as the temperature is lowered as expected. The bulk value  $C_B$  is proportional to  $\epsilon_{\perp}$ , the dielectric constant of the liquid crystal. From independent measurements<sup>13</sup>  $\epsilon_{\perp} \approx 5$  in the compound used in the present study and decreases with increase of temperature as required by Eq. (2). On the other hand, the boundary layer values  $R_{bl}$  and  $C_{bl}$  which are the lumped values from the polyamide coatings on both the electrodes hardly vary with temperature.

It is also easy to understand the higher effective dielectric constant exhibited by the thin cells compared to the thick one (Fig. 3). The ions move faster under the higher field acting in the thin cell, and also as the transit distance is shorter, the space charge contribution to the polarization is relatively large. Consequently, the effective dielectric constant goes up. This is reflected in Eq. (10) in which  $A \propto d$  occurs in the denominator of the expression for  $\epsilon'_l(\omega)$ . From that equation, the ionic contribution is also  $\propto nD^{3/2}$ . As the number density as well as the diffusion coefficient increase with temperature (see Table Ia),  $\epsilon'_l(\omega)$  increases with temperature, and compensates for the decrease of  $\epsilon_{\perp}$  with temperature reflecting that of the order parameter  $S$  as given by Eq. (2). The consequence is that the effective dielectric constant remains practically independent of temperature over a wide range (see Fig 3).

#### IV. CONCLUSIONS

Our experiments have shown that as the thickness of the cell is reduced to  $\sim 1-2 \mu\text{m}$ , the ionic contribution to the

dielectric response of a liquid crystal cell can be significant for samples with a conductivity  $\sim 10^{-10} (\Omega \text{ cm})^{-1}$ . The effect grows very large [ $\propto \omega^{-3/2}$  for the real part and  $\propto \omega^{-1}$  for the imaginary part, see Eqs. (10) and (11)] as the frequency is reduced. In our simplified analysis, we have used the approximation that the nonuniformity of the electric field inside the cell arising from space charges can be ignored. The resulting simplified expressions for  $\epsilon'_l(\omega)$  and  $\epsilon''_l(\omega)$  reproduce the experimental data semiquantitatively even for the thin cell at high temperatures. Liquid crystals which are used in very thin display devices have to be highly purified to avoid the ionic contribution to the dielectric response and hence to the electro-optic characteristics. Indeed the nonuniform field arising from the space charge effects can be expected to alter the Freedericksz threshold voltage for materials with positive dielectric anisotropy. We have conducted some preliminary experiments to find this to be the case. These results along with the relevant analysis will be published elsewhere.

<sup>1</sup>P. G. de Gennes and J. Prost, *The Physics of Liquid Crystals*, 2nd ed. (Clarendon, Oxford, 1993).

<sup>2</sup>*Liquid Crystals: Applications and Uses*, edited by B. Bahadur (World Scientific, Singapore, 1990), Vol. 1.

<sup>3</sup>S. T. Lagerwall, *Ferroelectric and Antiferroelectric Liquid Crystals* (Wiley, Weinheim, 1999).

<sup>4</sup>T. Z. Qian, Z. L. Xie, H. S. Kwok, and P. Sheng, *Appl. Phys. Lett.* **71**, 596 (1997).

<sup>5</sup>J. X. Guo and H. S. Kwok, *Jpn. J. Appl. Phys., Part 1* **39**, 1210 (2000).

<sup>6</sup>R. N. Thurston, J. Cheng, R. B. Meyer, and G. D. Boyd, *J. Appl. Phys.* **56**, 263 (1984).

<sup>7</sup>G. Jaffe, *Phys. Rev.* **85**, 354 (1952).

<sup>8</sup>R. J. Friauf, *J. Chem. Phys.* **22**, 8 (1954).

<sup>9</sup>J. R. Macdonald, *Phys. Rev.* **92**, 1 (1953).

<sup>10</sup>S. Uemura, *J. Polym. Sci.* **10**, 2155 (1972).

<sup>11</sup>A. Sawada, K. Tarumi, and S. Naemura, *Jpn. J. Appl. Phys., Part 1* **38**, 1418 (1999).

<sup>12</sup>A. Sawada, H. Sato, A. Manabe, and S. Naemura, *Jpn. J. Appl. Phys., Part 1* **39**, 3496 (2000).

<sup>13</sup>B. S. Srikanta and N. V. Madhusudana, *Mol. Cryst. Liq. Cryst.* **103**, 111 (1983).

<sup>14</sup>G. Bassapa and N. V. Madhusudana, *Mol. Cryst. Liq. Cryst.* **288**, 161 (1996).